Available online at www.sciencedirect.com
ScienceDirect
Electrical Power and Energy Systems 29 (2007) 565–570
ELECTRICAL POWER & ENERGY SYSTEMS
www.elsevier.com/locate/ijepes

A nonlinear control for enhancing HVDC light transmission system stability

Si-Ye Ruan [a], Guo-Jie Li [a], Lin Peng [a], Yuan-Zhang Sun [a], T.T. Lie [b,*]

[a] State Key Laboratory of Power System, Tsinghua University, Beijing, PR China
[b] School of EEE, Nanyang Technological University, Singapore

Received 22 March 2005; accepted 8 January 2007

Abstract

The purpose of this paper is to study the mathematical model and its control strategy of HVDC Light transmission system in order to enhance system stability. In this paper, the steady state mathematical model for the HVDC Light system is developed and the decoupled relationship between the controlling variables is proposed. An appropriate controller utilizing nonlinear control for HVDC Light system is proposed to maintain the dc link voltage and control the active and reactive power. The control is not complex. Basic functions of HVDC Light system can be realized. What is further, better performances are obtained when compared with a traditional control. The digital simulation results show that the proposed nonlinear control is effective to damp system oscillations and enhance system stability.

Keywords: HVDC light; Nonlinear control; Digital simulation; PWM

1. Introduction

The past five decades witnessed significant development in high voltage direct current (HVDC) electrical power transmission system, which is continuously innovated by utilizing state-of-the-art power electronic devices. Most of these transmission systems are based on current source converters (CSC) utilizing thyristor technology. The shortcoming of this transmission technology is that the valve, thyristor, cannot be turned off with gate signal directly. That limits the range of its application.

In the recent year, rapid advancement is achieved in the field of power electronic devices which can not only switch on but also switch off immediately, such as insulated gate bipolar transistor (IGBT). That opens the opportunities for the power industry via the utilization of HVDC light [1–5], which is based on voltage sourced converters (VSC) with IGBT technology. Owing to IGBT valves, this new innovative technology exhibits substantial technical and economical advantages over conventional CSC-based HVDC transmission system. The benefits include: (i) active and reactive power exchange can be controlled flexibly and independently; (ii) no commutation failure problem; (iii) No communication required between two stations, and etc. [4].

To ensure the stable operation of HVDC Light transmission system, many research works about its control strategy have been carried out. Sinusoidal phase width modulation (SPWM) technology is now widely employed. SPWM modulator is constructed by comparing a low frequency sinusoidal with a unity amplitude triangular carrier. The sine wave signal holds two degrees of freedom, i.e., phase and amplitude. On the basis of it, phase and amplitude control (PAC) technology is developed [6,7]. The problem for this technology is that it is not easy to realize the decoupled control of real and reactive power. To solve this problem, a decoupled PI control of real and reactive power for HVDC Light system has been proposed in [9].

* Corresponding author. Tel.: +65 790 4519; fax: +65 6791 2687.
E-mail address: ettlie@ntu.edu.sg (T.T. Lie).

0142-0615/$ - see front matter © 2007 Elsevier Ltd. All rights reserved.
doi:10.1016/j.ijepes.2007.01.008

In this paper, a nonlinear feedback linearization control [8,10] is introduced into the HVDC Light transmission system. A steady-state model of HVDC Light system is firstly developed, and then it is transformed into d-axis and q-axis in rotating synchronous frame. According to this model, the corresponding relationship between the two control inputs and the two controlled variables of each station is determined. System stability is improved with the proposed control method. The validity of the steady-state model and the proposed control strategy is verified in EMTDC/PSCAD simulation environment.

The rest of the paper is organized as follows. In Section 2, the modeling of HVDC Light system is presented. In Section 3, the nonlinear PWM control is developed and discussed. Simulation results are presented and illustrated in Section 4. At last, Conclusions are drawn in Section 5.

2. Modeling of HVDC light system

There are two converter stations in the system. Each station shown in Fig. 1 is coupled with AC network via equivalent converter impedances R_1+jX_1 and R_2+jX_2. DC capacitors C_1 and C_2 ($C_1 = C_2 = C$) are used across DC side. It is assumed that AC networks at the terminal are very strong. Hence, they are modeled as the AC sources in the paper. It is possible because most of HVDC Light systems' capacities are relatively small when compared with that of power system [11]. What is more, three-phase line-to-line voltages are assumed to be well balanced.

Each VSC has 2 degrees of freedom. The reactive modulation of each VSC will use up one degrees. The other degree is used to control the real power or dc voltage. The real power modulation is applied in Inverter Station, while the dc voltage modulation is proposed in Rectifier Station to maintain power balance, as described in (7). In this paper, Station 1 is chosen as Rectifier station while Station 2 is designated as Inverter station.

The following equations indicate the relationships among different variables of the system [8].

Rectifier station:

$$\frac{\mathrm{d}i_{d1}}{\mathrm{d}t} = -\frac{R}{L}i_{d1} + \omega i_{q1} + u_{d1} \tag{1}$$

$$\frac{\mathrm{d}i_{q1}}{\mathrm{d}t} = -\omega i_{d1} - \frac{R}{L}i_{q1} + u_{q1} \tag{2}$$

$$\frac{\mathrm{d}v_{\mathrm{dc1}}}{\mathrm{d}t} = \frac{3u_{sq1}i_{q1}}{2Cv_{\mathrm{dc1}}} - \frac{i_L}{C} \tag{3}$$

where $u_{q1} = \frac{u_{sq1}-u_{rq1}}{L}$, $u_{d1} = \frac{u_{sd1}-u_{rd1}}{L}$

Inverter station:

$$\frac{\mathrm{d}i_{d2}}{\mathrm{d}t} = -\frac{R}{L}i_{d2} + \omega i_{q2} + u_{d2} \tag{4}$$

$$\frac{\mathrm{d}i_{q2}}{\mathrm{d}t} = -\omega i_{d2} - \frac{R}{L}i_{q2} + u_{q2} \tag{5}$$

$$\frac{\mathrm{d}v_{\mathrm{dc2}}}{\mathrm{d}t} = \frac{3u_{sq2}i_{q2}}{2Cv_{\mathrm{dc2}}} + \frac{i_L}{C} \tag{6}$$

where $u_{q2} = \frac{u_{sq2}-u_{rq2}}{L}$, $u_{d2} = \frac{u_{sd2}-u_{rd2}}{L}$

Interconnected relationship between Rectifier station and Inverter Station is:

$$v_{\mathrm{dc1}}i_L = v_{\mathrm{dc2}}i_L + 2R_0i_L^2 \tag{7}$$

In the synchronous frame, u_{sd1}, u_{sd2}, u_{sq1} and u_{sq2} are the d, q axes components of the respective source voltages, i_{d1}, i_{d2},i_{q1} and i_{q2} are that of the line currents, u_{rd1}, $u_{rd2}u_{rq1}$ and u_{rq2} are that of the converter input voltages. P_1, P_2, Q_1 and Q_2 are real and reactive power transferred from the network to the station. v_{dc1} and v_{dc2} are the DC bus voltages. i_L is the load current.

At the side of Station 1, the q-axis is set to be in phase with the source voltage U_{s1}. Correspondingly, the q-axis is set to be in phase of the source voltage U_{s2} at the side of Station 2. Therefore, u_{sd1} and u_{sd2} are equal to 0 while u_{sq1} and u_{sq2} are equal to the magnitude of u_{s1} and u_{s2}, which will simplify the following discussion.

Then the power flows from the sources can be given

$$P_1 = \frac{3}{2}(u_{sq1}i_{q1} + u_{sd1}i_{d1}) = \frac{3}{2}u_{sq1}i_{q1} \tag{8}$$

$$Q_1 = \frac{3}{2}(u_{sq1}i_{d1} - u_{sd1}i_{q1}) = \frac{3}{2}u_{sq1}i_{d1} \tag{9}$$

$$P_2 = \frac{3}{2}(u_{sq2}i_{q2} + u_{sd2}i_{d2}) = \frac{3}{2}u_{sq2}i_{q2} \tag{10}$$

$$Q_2 = \frac{3}{2}(u_{sq2}i_{d2} - u_{sd2}i_{q2}) = \frac{3}{2}u_{sq2}i_{d2} \tag{11}$$

The model of the HVDC Light system is based on (1)–(6) and a number of assumptions, from which the following discussions can proceed. To have the discussions validated, it will be necessary to build models of the converters for testing. Short of building real-life models, simulation studies are made through the PSCAD/EMTDC software package in the paper.

3. Nonlinear control design of HVDC light system

3.1. Rectifier control design

Without loss of generality, Station 1 is chosen as the rectifier and Station 2 the inverter. In Station 1, there are two

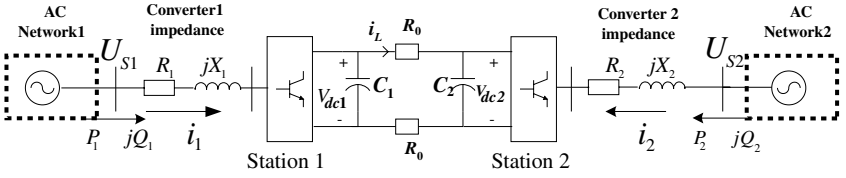

Fig. 1. Physical model of HVDC Light system.

controlled variables: the reactive power Q_1 and DC-bus voltage v_{dc1}. From (1)–(3), a mathematical model for rectifier station 1 can be described as follows:

$$\dot{x}_r = f_r(x) + g_r u_r \tag{12}$$

where

$$x_r = \begin{bmatrix} i_{d1} \\ i_{q1} \\ v_{dc1} \end{bmatrix}, \quad f_r(x) = \begin{bmatrix} f_{r1} \\ f_{r2} \\ f_{r3} \end{bmatrix} = \begin{bmatrix} -\frac{R}{L} i_{d1} + \omega i_{q1} \\ -\omega i_{d1} - \frac{R}{L} i_{q1} \\ \frac{3u_{sq1} i_{q1}}{2Cv_{dc1}} - \frac{i_L}{C} \end{bmatrix},$$

$$g_r = \begin{bmatrix} 1/L & 0 \\ 0 & 1/L \\ 0 & 0 \end{bmatrix}, \quad u_r = \begin{bmatrix} u_{r1} \\ u_{r2} \end{bmatrix} = \begin{bmatrix} u_{sd1} - u_{rd1} \\ u_{sq1} - u_{rq1} \end{bmatrix}.$$

From (12), it is clear that the system is of third order and has two control inputs.

Since some variables directly influence the system performance, their effects must be quickly behaved in the feedback control law. Therefore, the output can be chosen as

$$y_1 = i_{d1} \tag{13}$$

$$y_2 = v_{dc1} \tag{14}$$

To obtain an input–output linearization, differentiating (13) and (14) until the direct relationship between the outputs and inputs of the model can be readily obtained.

$$\begin{bmatrix} \dot{y}_1 \\ \ddot{y}_2 \end{bmatrix} = B_r + A_r \begin{bmatrix} u_{r1} \\ u_{r2} \end{bmatrix} \tag{15}$$

where

$$B_r = \begin{bmatrix} f_{r1} \\ \frac{3u_{sq1}}{2Cv_{dc1}} f_{r2} - \frac{3u_{sq1} i_{q1}}{2Cv_{dc1}^2} f_{r3} - \frac{i_L}{C} \end{bmatrix}, \quad A_r = \begin{bmatrix} 1/L & 0 \\ 0 & \frac{3u_{sq1}}{2CLv_{dc1}} \end{bmatrix}$$

Then the system's feedback form can be obtained:

$$\begin{bmatrix} v_{r1} \\ v_{r2} \end{bmatrix} = B_r + A_r \begin{bmatrix} u_{r1} \\ u_{r2} \end{bmatrix} \tag{16}$$

where $v_{r1} = \dot{y}_1, v_{r2} = \ddot{y}_2$

To achieve asymptotic tracking and robust control to parameter perturbation [8], the control inputs can be expressed by the followings.

$$\begin{bmatrix} v_{r1} \\ v_{r2} \end{bmatrix} = \begin{bmatrix} \dot{y}_{1\mathrm{ref}} - k_{11} e_{r1} - k_{12} \int e_{r1} \mathrm{d}t \\ \ddot{y}_{2\mathrm{ref}} - k_{21} \dot{e}_{r2} - k_{22} e_{r2} - k_{23} \int e_{r2} \mathrm{d}t \end{bmatrix} \tag{17}$$

As a result, the error dynamics can be obtained as

$$\ddot{e}_{r1} + k_{11} \dot{e}_{r1} + k_{12} e_{r1} = 0$$

$$e_{r2} + k_{21} \ddot{e}_{r2} + k_{22} \dot{e}_{r2} + k_{23} e_{r2} = 0$$

where $e_{r1} = i_{d1} - i_{d1\mathrm{ref}}$ $e_{r2} = v_{dc1} - v_{dc1\mathrm{ref}}$

From (9), $i_{d1\mathrm{ref}}$ can be got as $i_{d1\mathrm{ref}} = \frac{2Q_{1\mathrm{ref}}}{3u_{sq1}} Q_{1\mathrm{ref}}$ and $v_{dc1\mathrm{ref}}$ are the reference values for Q_1 and v_{dc1}.

By placing the desired pole locations in the left half plane, the controller gains can be chosen through the pole placement technique.

Finally, the feedback law can be determined.

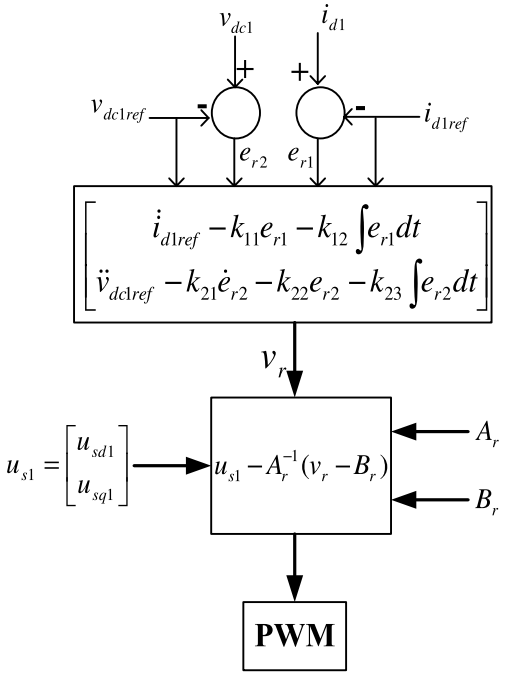

Fig. 2. Block diagram of nonlinear design for Rectifier station.

$$\begin{bmatrix} u_{r1} \\ u_{r2} \end{bmatrix} = A_r^{-1} \left(\begin{bmatrix} v_{r1} \\ v_{r2} \end{bmatrix} - B_r \right) \tag{18}$$

Its diagram is given in Fig. 2.

3.2. Inverter control design

Correspondingly, Station 2 is dedicated to the control of the reactive power Q_2 and active power P_2. For the Inverter station, it is usually considered that its dc voltage is constant. So its state equations are of second order and two inputs.

$$\dot{x}_i = f_i(x) + g_i u_i \tag{19}$$

where

$$x_i = \begin{bmatrix} i_{d2} \\ i_{q2} \end{bmatrix}, \quad f_i(x) = \begin{bmatrix} f_{i1} \\ f_{i2} \end{bmatrix} = \begin{bmatrix} -\frac{R}{L} i_{d2} + \omega i_{q2} \\ -\omega i_{d2} - \frac{R}{L} i_{q2} \end{bmatrix},$$

$$g_i = \begin{bmatrix} 1/L & 0 \\ 0 & 1/L \end{bmatrix}, \quad u_i = \begin{bmatrix} u_{i1} \\ u_{i2} \end{bmatrix} = \begin{bmatrix} u_{sd2} - u_{rd2} \\ u_{sq2} - u_{rq2} \end{bmatrix}$$

where u_{sd2}, u_{sq2}, u_{rd2}, u_{rq2}, i_{d2} and i_{q2} are electrical parameters at the side of Station 2.

Then, the output can be selected as

$$w_1 = i_{d2} \tag{20}$$

$$w_2 = i_{q2} \tag{21}$$

The following deductions are similar to that in Station 1. The control inputs can be expressed by the followings.

$$\begin{bmatrix} v_{i1} \\ v_{i2} \end{bmatrix} = \begin{bmatrix} \dot{w}_{1\mathrm{ref}} - k_{31} e_{i1} - k_{32} \int e_{i1} \mathrm{d}t \\ \dot{w}_{2\mathrm{ref}} - k_{41} e_{i2} - k_{42} \int e_{i2} \mathrm{d}t \end{bmatrix} \tag{22}$$

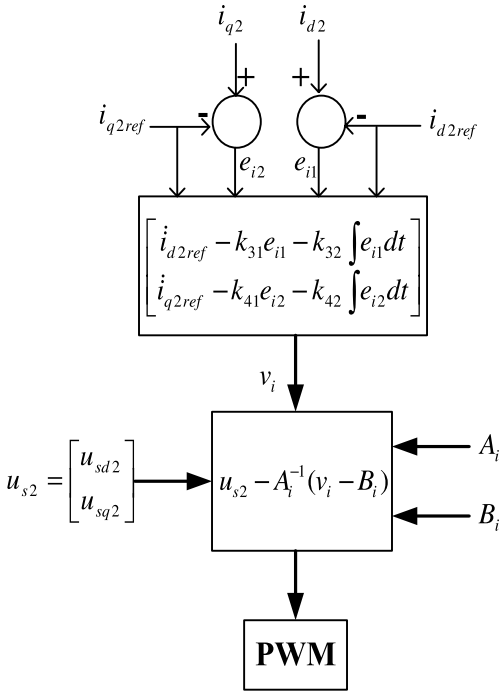

Fig. 3. Block diagram of nonlinear design for Inverter station.

where

$$e_{i1} = i_{d2} - i_{d2\text{ref}}, e_{i2} = i_{q2} - i_{q2\text{ref}}, i_{d2\text{ref}} = \frac{2Q_{2\text{ref}}}{3u_{sq2}} i_{q2\text{ref}} = \frac{2P_{2\text{ref}}}{3u_{sq2}}$$

In the end, the feedback law can be obtained

$$\begin{bmatrix} u_{i1} \\ u_{i2} \end{bmatrix} = A_i^{-1}\left(\begin{bmatrix} v_{i1} \\ v_{i2} \end{bmatrix} - B_i\right) \tag{23}$$

where

$$B_i = \begin{bmatrix} f_{i1} \\ f_{i2} \end{bmatrix}, \quad A_i = \begin{bmatrix} 1/L & 0 \\ 0 & 1/L \end{bmatrix}$$

In the above sections, $Q_{2\text{ref}}$ and $P_{2\text{ref}}$ are the reference values for Q_2 and P_2.

Hence, the proposed control diagram for Inverter station is shown in Fig. 3.

4. Simulation results

To validate the established steady-state model and the proposed control strategy, simulation studies of the system shown in Fig. 1 have been done with digital simulation software package PSCAD/EMTDC. The simulation conditions are as follows:

Input voltage: $U_{s1} = U_{s2} = 10$ kV
AC line resister: $R_1 = R_2 = 0.05\ \Omega$
AC line reactor: $L_1 = L_2 = 2.3$ mH
DC capacitor: $C_1 = C_2 = 500\ \mu F$
DC line resister: $R_0 = 0.1\ \Omega$

The rated dc voltage is 16 kV. The rated capacity of each station is 3 MVA. A 1600 Hz of moderate switching frequency is adopted in the simulations.

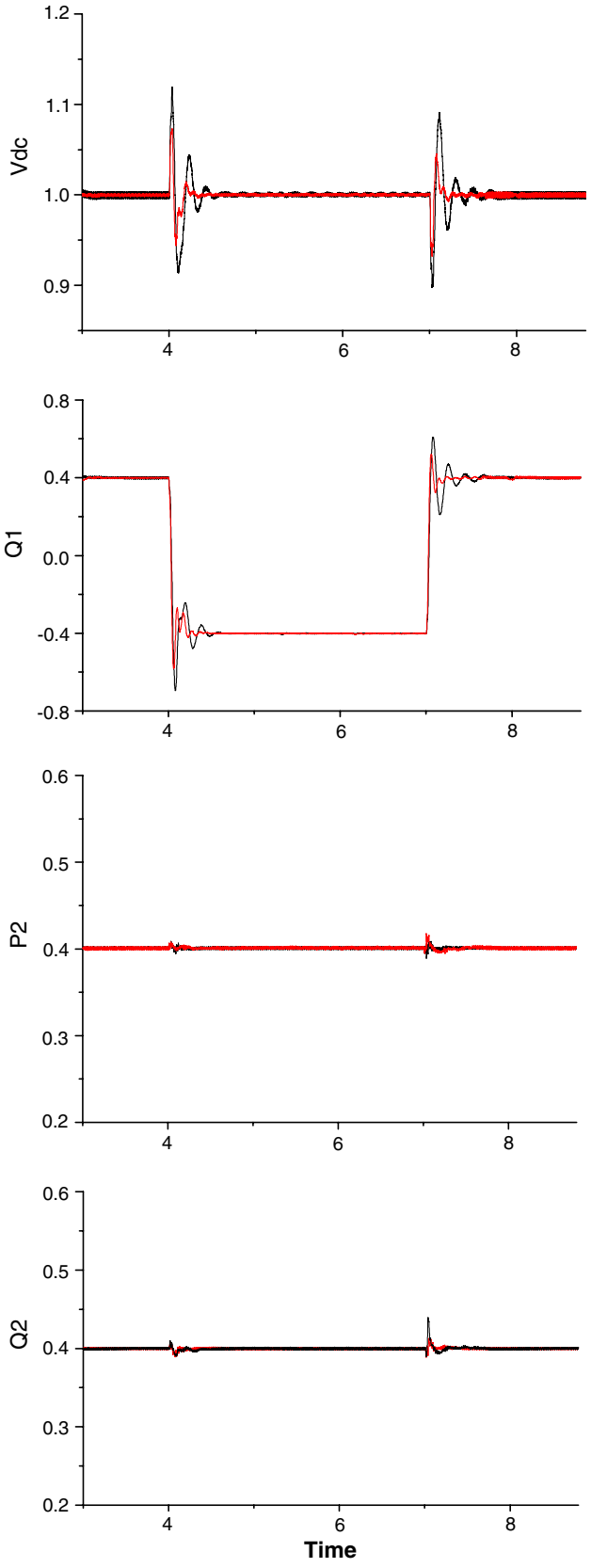

Fig. 4. System responses when Q1 is reversed.

To test the effectiveness of the nonlinear control, the system responses during the power reversion of the reactive Q_1 and the real power P_2 are demonstrated through the digital

simulation, from which it can be verified whether the proposed control can deal with the large regulation of power flow. This method is usually adopted to test the control system of HVDC light [6,11]. The simulation results are shown in Figs. 4 and 5. The case to change the value of Q_2 is not given because it is similar to that of Q_1. It is noted that all those variables are expressed in per unit values. In order to show the advantages of the nonlinear control, the results under the conventional PI control are also given. Then comparisons are made between these two controls:

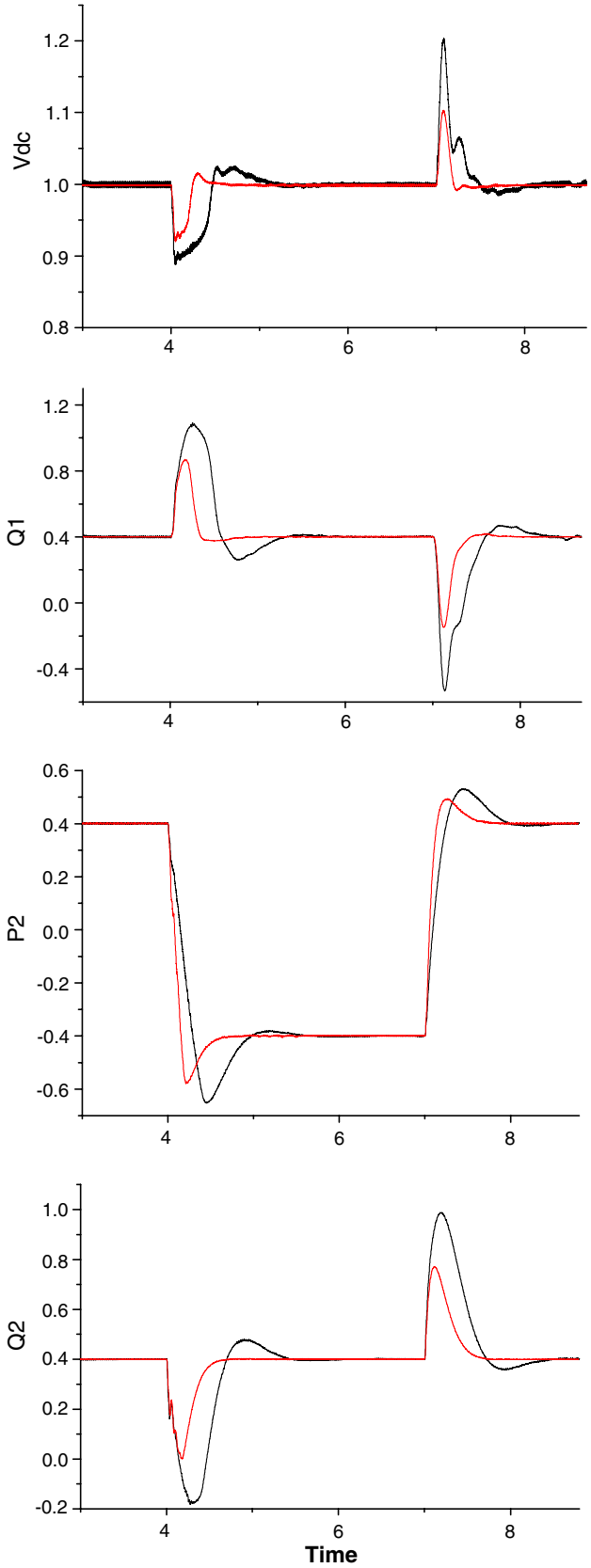

Fig. 5. System responses when P2 is reversed.

Control 1. Conventional PI control in rotating synchronous frame, which is in black curve.

Control 2. Nonlinear control in rotating synchronous frame, which is in red curve.

The system response with the reversion of reactive power is given in Fig. 4. The reference value for Q_1 changes from +0.4 to −0.4 at 4 s, then changes back at 7 s. The HVDC Light system under two different controls can both reach new operating points when Q_1 changes. However, control 2 proposed in this paper is faster to damp the oscillations than control 1. Take the behaviour of DC voltage for example. The moment Q_1 changes from +0.4 to –0.4, there is DC voltage fluctuation ranging from 0.95 p.u to 1.075 p.u with control 2, which only takes 0.3 s to be stable. By contraries, there is DC voltage fluctuation ranging from 0.91 p.u to 1.12 p.u with control 1, which takes 1 s to be stable. As regards to P_2 and Q_2, the change of Q_1 does not affect them too much.

Fig. 5 demonstrates the system performances while the real power changes. P_2 changes from 0.4 p.u to −0.4 p.u at 4 s, and turns back at 7 s. Compared with reactive power, the impact of real power to the system is much more serious. It is because variation of real power affects the dc voltage. And dc voltage is related to the converter input voltage [7], which is also the input of the nonlinear control. Considering the moment that reference value of P_2 changes from 0.4 p.u to –0.4 p.u, a big drop of DC voltage occurs. The DC voltage does not recover as quickly as that in Fig. 4. The DC voltage drops to 0.93 p.u and takes 0.6 s to be stable by control 2 while it drops to 0.88 p.u and takes 1.5 s to be stable by control 1. The reversion of P_2 also greatly impacts Q_1 and Q_2.

From Figs. 4 and 5, it is obvious that nonlinear control is very successful. First of all, this control can be applied to realize the basic functions of HVDC Light. It can control the active and reactive power independently and flexibly without changing control mode. And all of the feedback signals obtained are at the local side, as shown in (18) and (23), which means communication between two stations is not necessary during the normal power flow operation. It means that the cost of HVDC Light System can be reduced. Secondly, it improves the system behaviors when compared with conventional control. From Figs. 4 and 5, it is shown that the nonlinear control is more effective in damping oscillations and the system takes less time to be stable, which

also enhances HVDC Light System's stability. Thirdly, the control laws obtained is not complicated and it is all based on the local mode. Thus, it can be easily implemented into practice.

5. Conclusions

In this paper, the steady state of mathematical model for the HVDC Light system is developed and a nonlinear control is applied to the above system. The control performance has been compared with that of conventional control. Simulation results show that the nonlinear control is very effective. With the proposed control, power flow of HVDC Light system can be controlled flexibly and independently without changing control mode. System responses are improved when compared with the conventional control. What is more, the control law is not complex and it is all in the local mode. All of these merits make the nonlinear control strategy very practical.

Acknowledgement

This work was supported in part by the National Science Foundation of China under Grant 50377017.

References

[1] Andersen BR, Xu L, Horton PJ, Cartwright P. Topologies for VSC transmission. Power Eng J 2002;16 (June):142–50.
[2] Venkataramanan G, Johnson BK. A superconducting DC transmission system based on VSC transmission technologies. IEEE Trans Appl Supercond 2003;13 (June):1922–5.
[3] Jowder FAR, Ooi BT. VSC-HVDC station with SSSC characteristics. IEEE Trans Power Electron 2004;19 (July):1053–9.
[4] Weimers L. HVDC light: a new technology for a better environment. IEEE Power Eng Rev 1998;8 (August):19–20.
[5] Asplund G. Application of HVDC Light to power system enhancement. IEEE Power Eng Soc Winter Meet 2000;4 (January):2498–503.
[6] Zhang G, Xu Z. Steady-state model for VSC based HVDC and its controller design. IEEE Power Eng Soc Winter Meet 2001;3 (February):1085–90.
[7] Ooi BT, Wang X. Boost-type PWM HVDC transmission system. IEEE Trans Power Deliv 1991;6 (October):1557–63.
[8] Lee Dong-Choon, Lee Ki-Do, Lee G-Myoung. Voltage control of PWM converters using feedback linearization. In: Proceedings of the IEEE thirty-third IAS annual meeting, vol. 2, October 1998; p. 1491–6.
[9] Lu Weixing, Ooi BT. Multi-terminal DC transmission system for windfarms. IEEE Power Eng Soc Winter Meet 2001;3 (January):1091–6.
[10] Baik In-Cheol, Kim Kyeong-Hwa, Youn Myung-Joong. Robust nonlinear speed control of PM synchronous motor using boundary layer integral sliding mode control technique. IEEE Trans Contr Syst Technol 2000;8 (January):47–54.
[11] Bahrman MP, Johansson JG, Nilsson BA. Voltage source converter transmission technologies: the right fit for the application. IEEE Power Eng Soc Gen Meet 2003;3 (July):1840–7.